

KUNS-1351  
HE(TH) 95/11

# Parameter Bounds in the Supersymmetric Standard Model from Charge/Color Breaking Vacua

Andrew J. Bordner <sup>\*</sup>

*Department of Physics, Kyoto University, Kyoto 606-01, Japan*

(October 1, 2018)

## Abstract

We calculate limits on the trilinear soft-breaking parameter,  $A_t$ , in the Minimal Supersymmetric Standard model by requiring the absence of nonzero top squark vacuum expectation values. Assuming a low  $\tan\beta$ , which implies a large top Yukawa coupling, we also calculate one-loop corrections to the effective potential. The resulting numerical calculations of the charge/color breaking limits are presented as best-fit surfaces. We compare these results with the analytical limit,  $A_t^2 < 3(m_2^2 + m_{\tilde{q}}^2 + m_{\tilde{t}}^2)$ , and find that although this is a good estimate of the charge/color breaking bounds for a simplified model of the top sector, stricter bounds are found by a numerical minimization of the Minimal Supersymmetric Standard Model potential.

## I. INTRODUCTION

The Minimal Supersymmetric Standard Model (MSSM) may be described by a Lagrangian containing interactions consistent with invariance under the gauge group  $SU(3) \times$

---

<sup>\*</sup>e-mail address: bordner@gauge.scphys.kyoto-u.ac.jp

$SU(2) \times U(1)_Y$  and global supersymmetry plus a Lagrangian containing a restricted set of soft supersymmetry breaking terms [1]. These terms break supersymmetry while maintaining a useful property of a supersymmetric theory, namely the cancellation of quadratic divergences [2]. The absence of these divergences is necessary in order to define the renormalized mass of a fundamental scalar, such as the Higgs boson, without a fine-tuning of the cancellation between the bare mass and the scalar self-energy [3].

The presence of fundamental scalar fields in the MSSM, besides the Higgs bosons, leads to the possibility that these fields may acquire non-zero vacuum expectation values (vevs). Since this would violate the conservation of color and/or electric charge symmetry, this leads to forbidden regions of the parameter space of the theory. We will calculate numerical estimates of the boundary of the allowed region of soft-breaking parameters using both the tree-level potential and the one-loop effective potential.

Many studies of the MSSM mass spectrum neglect these charge/color breaking, or CCB, bounds in their analyses. Previously, CCB bounds were obtained for various supersymmetric models, however no systematic numerical study of CCB constraints for a realistic approximation to the MSSM using the one-loop effective potential has been done [4,5].

One may assume that there are relations among the soft breaking terms, such as in the minimal supergravity model in which all scalar masses and scalar trilinear couplings are the same at the unification scale, of order  $10^{16} \text{ GeV}$  [6]. However we will find constraints on the soft-breaking parameters at a low-energy scale,  $Q_0$ , with  $Q_0 < 1 \text{ TeV}$ . This is an indeterminate upper limit on particle masses if the MSSM is to explain the gauge hierarchy problem. We will not make any assumptions about the theory near the GUT scale nor the particle spectrum above  $Q_0$ .

We will use an approximation to the MSSM that includes only the top flavor supermultiplets. This follows from evidence that the top quark mass  $m_t \approx 176 \text{ GeV}$  [7]. We use the conventional definition  $\tan \beta \equiv v_2/v_1$ , with  $v_1, v_2$  the vevs for the Higgs scalar fields,  $H_1$  and  $H_2$ , respectively. Assuming a small value for  $\tan \beta$ , near 1.0, gives the top quark Yukawa coupling,  $h_t = 1.0$ . The contributions from the bottom supermultiplets may then

be ignored.

There are various reasons to choose these particular values of  $\tan\beta$  and to consider only the top squarks as acquiring a non-zero vev. First of all, there is an infrared quasi-fixed point in the renormalization group equation for  $h_t(Q)$  which corresponds to a value  $h_t^{FP}(m_t) \approx 1.25$  [8]. The mass relation

$$m_t(m_t) = \frac{h_t^{FP}(m_t)}{\sqrt{2}} v \sin\beta \quad (1)$$

gives  $\tan\beta \approx 1.2$  if one uses the relation between the top quark mass defined by the pole in its propagator and its running mass to first-order in the QCD gauge coupling [9].

$$m_{pole} = m_t(m_t) \left[ 1 + \frac{4}{3\pi} \alpha_3(m_t) + \mathcal{O}(\alpha_3^2) \right]. \quad (2)$$

Therefore a value of  $\tan\beta$  at  $Q_0$  in the range  $1.1 < \tan\beta < 2.0$  results from a large range of  $h_t$  values at the GUT scale. Although  $\tan\beta$  is not required to be in this range, it indicates that this is a natural choice. One motivation for considering only the top sector comes from assuming common soft-breaking parameters at the GUT scale. A large value of  $h_t$  causes the third generation parameters to undergo the largest change as they are evolved from  $Q_{GUT}$  down to  $Q_0$ . For this same reason,  $h_t$  also gives the largest contribution to the radiative gauge symmetry breaking of  $SU(2) \times U(1)_Y$  [10,11]. Therefore, if one assumes that the minimum of the effective potential at energy scales  $Q \gg Q_0$  gives zero vevs for the scalar fields, such as in the case of universality at the GUT scale, as one evolves to  $Q_0$  the third-generation parameters undergo the largest change and the CCB constraints from third generation scalar fields will be the most restrictive. Finally, as discussed in Ref. [12], the potential barrier height for tunneling from the symmetric vacuum at a high temperature ( $T > 100$  GeV), early in the expansion of the universe, to a lower CCB minimum is proportional to  $1/h_{min}^2$  where  $h_{min}$  is the smallest of the Yukawa couplings for the slepton and squark fields that have non-zero vevs at the CCB minimum. This implies that one should consider CCB vacua in which only the Higgs fields and the top squarks have non-zero vevs in order for the tunneling from the symmetric to the CCB vacuum to have occurred in a time less than the present age of the universe ( $\approx 10^{10}$  years).

## II. APPROXIMATION TO THE MSSM

We use a consistent approximation to the MSSM with  $\tan\beta = 1.5$  as a small value near the fixed point value and interactions with the bottom quark superfields are ignored. We use all MSSM interactions between the following fields  $H_1$ ,  $H_2$ ,  $\widetilde{H}_1$ ,  $\widetilde{H}_2$ ,  $q$ ,  $t^c$ ,  $\tilde{q}$ ,  $\tilde{t}^c$ ,  $A_\mu$ , and  $\lambda$ .  $H_1$  and  $H_2$  are respectively the hypercharge  $-1$  and  $+1$  Higgs boson doublets. The corresponding field variables with a tilde are the Higgsino doublets.  $q$  and  $t^c$  are the left-handed component of the top quark and the right-handed component of the charge conjugate top quark field respectively. Again, the corresponding field variables with tildes are the top squarks.  $A_\mu$  is the gluon field and  $\lambda$  is the gluino field. Notice that the field content in this approximation is supersymmetric. This arises from including all interactions with the top quark supermultiplet involving the parameters  $h_t$  and  $\mu$ . The potential in this approximation as well as the definitions of the parameters appearing in it are shown in the appendix.

We use the values of the gauge couplings at the weak scale  $M_Z$ :  $g_1 = 0.358$ ,  $g_2 = 0.652$ , and  $g_3 = 1.213$  for all calculations [13]. Since we will take the renormalization scale to be  $Q_0 = 500 \text{ GeV}$ , the running of the gauge couplings from  $M_Z$  to this scale is negligible. We also omit the couplings  $g_1$  and  $g_2$  in the calculation of the one-loop effective potential. However, we retain the terms with these couplings at tree-level since they include the quartic Higgs scalar interactions responsible for the non-zero Higgs vev of the Standard Model (SM).

## III. THE EFFECTIVE POTENTIAL

Quantum corrections may affect whether spontaneous symmetry breaking occurs in a field theory. The vevs of the scalar fields are the values of the classical fields at the minimum of the effective potential. We use the one-loop correction to the effective potential in the dimensional reduction,  $\overline{DR}$ , renormalization scheme [14]

$$V_{eff}^{1-loop} = \frac{1}{64\pi^2} Str \left[ \mathcal{M}^4 \left( \ln \frac{\mathcal{M}^2}{Q^2} - \frac{3}{2} \right) \right], \quad (3)$$

where the supertrace,  $Str$ , is over all color and spin degrees of freedom with a minus sign for fermions.  $Q^2$  is the square of the renormalization scale, which we take to be equal to  $Q_0^2$ .  $\mathcal{M}^2$  is the field dependent mass matrix; for instance, for a theory with scalar fields  $\phi_i, i = 1, \dots, n$

$$\mathcal{M}_{ij} = \left. \frac{\partial^2 V}{\partial \phi_i \partial \phi_j} \right|_{\phi=\phi_c}. \quad (4)$$

$\mathcal{M}$  as well as  $V_{eff}$  are function of the classical fields  $(\phi_i)_c = \langle 0 | \phi_i | 0 \rangle$ . Since the top Yukawa coupling,  $h_t$ , and the strong gauge coupling,  $g_3$ , are large one may expect significant contributions to the effective potential from one-loop corrections. The one-loop effective potential is also more stable under a change of renormalization scale [11]. Since the parameters appearing in the equation for the one-loop correction to  $V_{eff}$  are the renormalized parameters we consider the resulting CCB constraints as being limits on these renormalized parameters in the  $\overline{MS}$  scheme at momentum scale  $Q_0$ . If large logs of ratios of massive parameters appear in the effective potential, such as  $\ln(m_i^2/m_j^2)$  or  $\ln(\phi_i^2/m_j^2)$ , then one may, in principle, sum these using the renormalization group equation [15]. However, this is difficult when there are multiple scalar fields and masses. We only consider masses,  $m_i$ , and the renormalization scale,  $Q_0$ , which differ by less than two orders of magnitude. Furthermore, since we are only interested in the effective potential near its minimum where  $(\phi_i)_c \sim m_j$ , i.e., the classical field near the minimum of  $V_{eff}$  is of the same order of magnitude as the masses, the logarithms appearing in  $V_{eff}$  are small. Renormalization group improvement of the effective potential in this case is unnecessary.

We also assume that the Lagrangian parameters are real. In a field basis where the Higgs fields are real and positive and  $h_t$  and the scalar masses,  $m_i^2$ , real, only one of the parameters  $A_t$ ,  $\mu$ , or  $m_\lambda$  may be made real by redefining the fields. However, it was shown in Ref. [16] that the presence of complex phases in these parameters, greater than about  $10^{-2}$ , gives too large of a contribution to the neutron's electric dipole moment due to gluino loops.

#### IV. NUMERICAL CALCULATION

We evaluate the one-loop effective potential using Eq. (3) by diagonalizing the mass matrix  $\mathcal{M}$ . If one chooses the Landau gauge for the gluons, in which the propagator is

$$-\imath \left[ \frac{g_{\mu\nu} - k_\mu k_\nu}{k^2} \right] \frac{1}{k^2 + \imath\epsilon}, \quad (5)$$

the generalized mass matrix  $\mathcal{M}$  is block diagonal in the gluon fields, bosonic fields, and fermionic fields. The top squark fields may also be rotated by a global  $SU(3)$  transformation so that they are of the form

$$\tilde{q}_i = \begin{pmatrix} q_{1R} \\ 0 \\ 0 \end{pmatrix}, \quad \tilde{t^c}_i = \begin{pmatrix} t_{1R} + \imath t_{1I} \\ t_{2R} \\ 0 \end{pmatrix}, \quad (6)$$

with  $q_{1R}$ ,  $t_{1R}$ ,  $t_{1I}$ , and  $t_{2R}$  are real. We then use only the real part of the one-loop effective potential; the imaginary part is related to the decay rate of the vacuum as shown in Ref. [17].

The global minimum of the effective potential is found by calculating the local minimum using a standard algorithm from Ref. [18] starting from a set of field values on a rectangular grid. If this global minimum occurs for non-zero values of the squark fields then there is a CCB vacuum. This process is repeated for a set of soft-breaking parameter values on a rectangular grid in parameter space. A quadratic surface is then fit to the parameter points on the boundary between those that give a symmetric vacuum and those that lead to a CCB vacuum. The surface is fit to the boundary points by varying the coefficients in the equation of the surface,  $(P_1, \dots, P_8)$ , until the average of the distance squared from the boundary points to the nearest point on the surface,  $\langle d^2 \rangle$ , is minimized. The equation of the surface is

$$A_t^4 + P_1 A_t^2 + P_2 m_2^4 + P_3 m_2^2 + P_4 m_{\tilde{q}}^4 + P_5 m_{\tilde{q}}^2 + P_6 m_t^4 + P_7 m_t^2 - P_8 = 0 \quad (7)$$

with  $(A_t, m_2^2, m_{\tilde{q}}^2, m_t^2)$  a point in parameter space. These soft-breaking parameters are defined in the appendix. This particular parameterization of the surface is chosen solely because

of its simplicity, but as will be seen later it gives an accurate characterization of the CCB boundary.

Because of the large dimension of the parameter space in which we want to find CCB bounds, it is necessary to initially constrain some of the parameters values in order to reduce the calculation time. Two of the soft-breaking parameters,  $m_1^2$  and  $m_3^2$ , are constrained using two different methods. In method S the values of these parameters are chosen such that there is a Standard Model minimum in the effective potential with  $\langle \tilde{q} \rangle = \langle \tilde{t}^c \rangle = 0$  and  $\langle H_1 \rangle = v \cos \beta$ ,  $\langle H_2 \rangle = v \sin \beta$  with  $v = 246 \text{ GeV}$ . This is done by solving the analytical expression for the one-loop effective potential with zero vevs for the top squarks in terms of these parameters. These relations are shown in Eq. (22). In the other procedure, method F, we simply fix  $m_1^2$  and  $m_3^2$  at constant values, i.e., independent of the other soft-breaking parameters.

## V. RESULTS

### A. CCB Bounds for a Simplified Model

We begin with a numerical analysis of the model with three real scalar fields  $H$ ,  $Q$ , and  $T$  of Ref. [5]. The potential in this model is

$$\begin{aligned} h^2 V = & (Q^2 T^2 + Q^2 H^2 + T^2 H^2) - 2AQTH + m_Q^2 Q^2 \\ & + m_T^2 T^2 + m_H^2 H^2 + \frac{1}{8h^2} \left[ g_1^2 (H^2 + \frac{1}{3}Q^2 - \frac{4}{3}T^2)^2 \right. \\ & \left. + g_2^2 (H^2 - Q^2)^2 + \frac{4}{3}g_3^2 (Q^2 - T^2)^2 \right] \end{aligned} \quad (8)$$

This is a simplified version of the potential described in the appendix with  $Q = \tilde{q}$ ,  $T = \tilde{t}^c$ , and  $H = H_2^0$ . The CCB bound

$$A^2 < 3(m_2^2 + m_Q^2 + m_T^2), \quad (9)$$

derived in Ref. [5] follows from minimizing the potential only in the equal-field direction, *i.e.*,  $Q = T = H$ . This is valid, in general, only if the D-term dominates, or if  $g_i/h \gg 1$

with  $g_i$  the smallest gauge coupling.

We perform a numerical analysis of the potential in Eq. (8) using the parameter value ranges shown in Table I and with  $h = 0.1$ . The gauge couplings are fixed at their running values at the weak scale  $M_Z$  as stated earlier. The resulting best fit to the CCB boundary is shown in Table II. Clearly, this is close to the analytical result of Eq. (9), as it should be with a small value for  $h$ .

Next we repeat the analysis for the potential of Eq. (8) with the same soft-breaking parameter ranges of Table I, but we set  $h = 1.0$ . This is the proper value for the top quark Yukawa coupling for small  $\tan \beta$ . The corresponding CCB bound is given in Table II.

The CCB bound for  $h = 1.0$  is more stringent than the bound for  $h = 0.1$ , i.e., for a given set of parameter values within the range given in Table I,  $(m_2^2, m_{\tilde{q}}^2, m_{\tilde{t}}^2)$ , the value of the  $A$  parameter at which the vacuum becomes CCB is lower. The fractional difference in the  $A$  parameter bound between these cases is largest when the other parameters,  $(m_2^2, m_{\tilde{q}}^2, m_{\tilde{t}}^2)$ , are near the lower end of their range in Table I, where  $\Delta A/A \approx 15$ . Also the value of  $A$  at the CCB bound in this case is small. The average fractional difference over the entire parameter ranges shown in Table I for the two bounds is  $\Delta A/A \approx 0.14$

## B. CCB Bound for the MSSM

Next we examine the CCB bounds obtained from of our approximation to the MSSM with the Lagrangian given in the appendix. In all of the following analyses the mass units are  $TeV$ . We also fix  $\tan \beta = 1.5$  and  $\mu = 0.4$ . The renormalization scale for the one-loop calculation of the effective potential is set at  $Q = 0.5$ .

We first examine the bound for method F with  $m_1^2 = 0.65$  and  $m_3^2 = 0.40$ . These masses result in a value of  $m_2^2 = 0.26$  if a S.M. minimum were required, i.e., zero squark vevs. These values for  $m_1^2$  and  $m_3^2$  were chosen since they are consistent with a S.M. minimum for  $\tan \beta = 1.5$  and they are close to the renormalization scale,  $Q = 0.5$ . The ranges of parameter values for which the effective potential was calculated are shown in Table III.

The CCB bounds for the analyses of both the tree-level and the one-loop effective potential are shown in Table V. Parameter values which give a potential that is unbounded below are not used in determining the best fit surface for the CCB bound. This includes values with  $m_2^2 < 0.15$  for the tree-level potential since in this case the potential is unbounded for  $m_2^2 < 2m_3^2 - m_1^2$  and zero squark vevs. We do not examine negative  $m_2^2$  values since in this case, for the small range of  $m_q^2$  and  $m_t^2$  values for which the potential is bounded below, the vevs for the C.C.B. vacuum are too small for the numerical methods to distinguish this minimum from the minimum with all vevs vanishing. However, according to Eq. (21), the Higgs soft-breaking mass,  $m_{H2}^2$ , is negative over part of the parameter range examined.

Next we calculate the CCB bounds using method S, in which  $m_1^2$  and  $m_3^2$  are fixed by requiring a S.M. minimum. The parameter values listed in Table III were used in determining the bounds. Since there is no Standard Model minimum for  $m_2^2 < (60 \text{ GeV})^2$ , we do not examine  $m_2^2$  values in this range. The CCB bounds calculated by finding the global minimum of the both the tree-level potential and the one-loop effective potential are given in Table IV.

## VI. DISCUSSION

The quadratic surface of Eq. (7) is sufficient to provide an accurate characterization of the numerical CCB bound. All of the least-square fits give the average distance squared,  $\langle d^2 \rangle \leq 1.0 \times 10^{-2}$ . The one-loop CCB bound calculations yield a larger value for  $\langle d^2 \rangle$  because the longer calculation time requires using less parameter grid points than for the tree-level calculation. Typically it takes around 20 days of cpu time on a Digital Alpha workstation to calculate the one-loop CCB boundary points and perform a least-squares fit so we are limited by the computation time.

As stated in section V A, the numerical CCB bound for the simplified Lagrangian of Ref. [5] with Yukawa coupling  $h = 1.0$  is significantly different from the numerical bound with  $h = 0.1$ , and hence also different from the analytical bound of Eq. (9), when the other

soft-breaking parameters are small. However, for the remainder of the parameter values tested, the numerical bound with  $h = 1.0$  is quite close to the analytical bound. One would not expect the CCB bound of Eq. (9) to be correct for large  $h$ . One possible explanation is that the  $g_3^2$  D-term is large enough at least to insure that the minimum is in the direction  $Q = T$ . Also for  $h = 1.0$  the numerical bound does give a more stringent CCB bound than that of Eq. (9) over the entire range of parameters tested.

We present some contour plots of the CCB bounds with  $m_2^2 = 0.25$  for comparison. The contours show the value of  $A_t$  on the CCB boundary, i.e., lower values of  $A_t$  result in a symmetric vacuum whereas higher values result in a CCB vacuum with nonzero squark vevs. Figs. 1 and 2 show the bounds for method F using the tree-level and one-loop effective potential respectively. Figs. 3 and 4 show the tree-level and one-loop method S CCB bounds. Fig. 5 shows the analytical bound of Eq. (9) with  $m_2^2 = 0.25$ .

Since there is not the additional constraint of requiring a Standard Model minimum for the Higgs field for both the method F CCB bounds and for the analytical bound, one may compare these CCB bounds. The tree-level CCB bound on the  $A_t$  parameter for method F is lower than the analytical bound of Eq. (9) for the entire range of parameter values,  $(m_2^2, m_{\tilde{q}}^2, m_{\tilde{t}}^2)$ , shown in Table III. The one-loop correction to the effective potential raises the value of  $A_t$  for the CCB bound over about 70% of the parameter range considered. However, even with the one-loop corrections, the CCB bound for the MSSM potential is more stringent, i.e., gives a lower value for  $A_t$ , than the bound of Eq. (9) for  $> 95\%$  of the parameter range.

The one-loop corrections for the CCB bound calculated using method S give a lower  $A_t$  value than the tree-level bound over the entire range of parameters examined. For values of the parameters,  $(m_2^2, m_{\tilde{q}}^2, m_{\tilde{t}}^2)$ , that give a small value for the  $A_t$  parameter CCB bound, the one-loop corrections to the effective potential makes the CCB bound significantly stricter.

In conclusion, CCB bounds on the soft-breaking parameters of the Higgs and top quark/squark sectors of the MSSM provide important constraints for these parameters. These constraints may be expressed as a maximum value of the  $A_t$  parameter for given

values of the remaining soft-breaking parameters. The numerical CCB constraints that we calculated give more stringent CCB bounds than the analytical constraint of Eq. (9) for most of the ranges of parameter values considered. Because of the large top Yukawa coupling, one-loop corrections to the effective potential may result in significantly different CCB bounds than those for the tree-level potential.

## ACKNOWLEDGEMENTS

The author wishes to thank Y. Okada for suggesting this topic and B. Wright for many useful discussions. This work was partially supported by the Japan Society for the Promotion of Science.

## APPENDIX

### Tree-level MSSM Potential

The potential may be divided into several parts. A sum over group and spinor indices, where applicable, is implied. The supersymmetric D-terms are

$$V_D = \frac{1}{8}g_1^2 \left( -H_1^\dagger H_1 + H_2^\dagger H_2 + \frac{1}{3}|\tilde{q}|^2 - \frac{4}{3}|\tilde{t}^c|^2 \right)^2 + \frac{1}{8}g_2^2 \sum_{a=1}^3 \left( H_1^\dagger \tau_a H_1 + H_2^\dagger \tau_a H_2 + \tilde{q}^* \tau_a \tilde{q} \right)^2 + \frac{1}{2}g_3^2 \sum_{a=1}^8 \left( \tilde{q}^* T^a \tilde{q} - \tilde{t}^c{}^* T^{*a} \tilde{t}^c \right)^2, \quad (10)$$

where  $g_1$ ,  $g_2$ , and  $g_3$  are respectively the  $U(1)_Y$ ,  $SU(2)$ , and  $SU(3)$  couplings,  $\tau_a$  are the Pauli matrices and  $T^a$  are the antihermitian generators of  $SU(3)$ . Using the relations

$$\tau_{ij}^a \tau_{kl}^a = 2\delta_{il}\delta_{jk} - \delta_{ij}\delta_{kl} \quad (11)$$

and

$$T_{ij}^a T_{kl}^a = \frac{1}{2} \left( \delta_{il}\delta_{jk} - \frac{1}{3}\delta_{ij}\delta_{kl} \right) \quad (12)$$

the  $SU(2)$  contribution becomes

$$\begin{aligned} V_{SU(2)} = & \frac{1}{8}g_2^2 \left[ (H_1^\dagger H_1)^2 + (H_2^\dagger H_2)^2 + (\tilde{q}^\dagger \tilde{q})^2 \right. \\ & - 2 \left( (H_1^\dagger H_1)(H_2^\dagger H_2) + (H_1^\dagger H_1)(\tilde{q}^\dagger \tilde{q}) + (H_2^\dagger H_2)(\tilde{q}^\dagger \tilde{q}) \right) \\ & \left. + 4 \left( |H_1^\dagger H_2|^2 + |H_1 \tilde{q}|^2 + |H_2^\dagger \tilde{q}|^2 \right) \right] \end{aligned} \quad (13)$$

and the  $SU(3)$  one is

$$V_{SU(3)} = \frac{1}{2}g_3^2 \left[ \frac{1}{3}(\tilde{q}^\dagger \tilde{q})^2 + \frac{1}{3}(\tilde{t}^c)^\dagger \tilde{t}^c - (\tilde{q} \tilde{t}^c)^\dagger (\tilde{q} \tilde{t}^c) + \frac{1}{3}(\tilde{q}^\dagger \tilde{q})(\tilde{t}^c)^\dagger \tilde{t}^c \right]. \quad (14)$$

The superpotential or F term is

$$V_F = h_t^2 \left( |\tilde{q}|^2 |H_2^0|^2 + |\tilde{t}^c|^2 |H_2^0|^2 + |\tilde{q} \tilde{t}^c|^2 \right) + h_t \mu (\tilde{q} \tilde{t}^c H_1^{0*}) + h.c., \quad (15)$$

with *h.c.* denoting the Hermitian conjugate and  $H_1^0$  and  $H_2^0$  are the neutral components of the Higgs scalar doublets. The Higgs scalar and fermion doublet components are

$$H_1 = \begin{pmatrix} H_1^0 \\ H_1^- \end{pmatrix}, \quad H_2 = \begin{pmatrix} H_2^+ \\ H_2^0 \end{pmatrix}. \quad (16)$$

The quark-squark-gluino interaction terms are

$$V_{q\tilde{q}\lambda} = \imath\sqrt{2}g_3 \left( \bar{t}P_L \lambda^{(a)} T^a \tilde{t}^{c*} - \tilde{t}^c T^a \bar{\lambda}^{(a)} P_R t + \tilde{q}^* T^a \bar{\lambda} P_L t - \bar{t} T^a \tilde{q} P_R \lambda^{(a)} \right). \quad (17)$$

$P_{L,R}$  are the projection operators for left- and right-handed chiral spinors,  $\frac{1}{2}(1 \pm \gamma^5)$ ,  $t$  is the four component spinor field for the top quark, and  $\lambda^{(a)}$  are the Majorana gluino fields. The quark-squark-Higgsino terms are

$$V_{q\tilde{q}\tilde{H}} = h_t \left( \tilde{t}^c \tilde{H}_2^0 P_L t + \tilde{t}^{c*} \bar{t} P_R \tilde{H}_2^0 - \tilde{q} \bar{t} P_L \tilde{H}_2^0 - \tilde{q}^* \tilde{H}_2^0 P_R t \right). \quad (18)$$

The Higgsino interaction terms are

$$V_{\tilde{H}\tilde{H}} = \mu \left( \tilde{H}_1^0 \tilde{H}_2^0 - \tilde{H}_1^- \tilde{H}_2^+ \right) + h.c. \quad (19)$$

Finally the SUSY soft-breaking terms are

$$\begin{aligned}
V_{soft-breaking} = & m_{H1}^2 H_1^\dagger H_1 + m_{H2}^2 H_2^\dagger H_2 - m_3^2 \epsilon_{ab} H_1^a H_2^b \\
& + m_{\tilde{q}}^2 |\tilde{q}|^2 + m_{\tilde{t}}^2 |\tilde{t}^c|^2 + \frac{1}{2} m_\lambda \bar{\lambda}^{(a)} \lambda^{(a)} + h_t A_t \tilde{q} \tilde{t}^c H_2^0 + h.c.
\end{aligned} \tag{20}$$

With the addition of the supersymmetric Higgs interactions, the masses for  $H_1$  and  $H_2$  become

$$m_1^2 = m_{H1}^2 + \mu^2 \tag{21}$$

$$m_2^2 = m_{H2}^2 + \mu^2$$

respectively.

### One-loop Effective Potential with Zero Squark VEVs

If the squark vevs are zero the one-loop contributions to the Higgs effective potential from top squark and quark loops may be written in an analytical form [19]. After requiring that the minimum of the effective potential be at  $H_1 = v_1$  and  $H_2 = v_2$  and solving for  $m_1^2$  and  $m_3^2$  we obtain

$$\begin{aligned}
m_3^2 = & (m_2^2 - m_Z^2 \cos 2\beta) \tan \beta \tag{22} \\
& + \frac{3}{16\pi^2} \left[ (h_t^2 A_t (A_t \tan \beta + \mu) \frac{f(m_2'^2) - f(m_1'^2)}{m_2'^2 - m_1'^2} \right. \\
& \left. + h_t^2 \tan \beta (f(m_1'^2) + f(m_2'^2) - 2f(m_t'^2)) \right], \\
m_1^2 = & m_3^2 \tan \beta - m_Z^2 \cos 2\beta \\
& + \frac{3}{16\pi^2} h_t^2 \mu (A_t \tan \beta + \mu) \frac{f(m_1'^2) - f(m_2'^2)}{m_2'^2 - m_1'^2},
\end{aligned}$$

with  $f(m^2) \equiv m^2(\ln(m^2/Q^2) - 1)$ . The definition  $\tan \beta = v_2/v_1$  and the tree-level Z boson mass,  $m_Z^2 = (v_1^2 + v_2^2)(g_1^2 + g_2^2)/4$ , were used. The tree-level relation follows by including only the first term in the above equations for  $m_1^2$  and  $m_3^2$ .

## REFERENCES

- [1] P. Fayet, Phys. Lett. B **69** (1977) 489; J. Rosiek, Phys. Rev. D **41** (1990) 3464.
- [2] L. Girardello, and M.T. Grisaru, Nucl. Phys. **B194** (1982) 65.
- [3] H.P. Nilles, Phys. Rep. **110** (1984) 1.
- [4] J.M. Frere, D.R.T. Jones, S. Raby, Nucl. Phys. **222** (1983) 11; L. Alvarez-Gaumé, J. Polchinski, M.B. Wise, *ibid.* **221** (1983) 495; C. Kounnas, A.B. Lahanas, D.V. Nanopoulos, M. Quiros, *ibid.* **236** (1984) 438; J.P. Derendinger and C.A. Savoy, *ibid.* **237** (1984) 307; H. Komatsu, Phys. Lett. B **215** (1988) 323; P. Langacker and N. Polonsky, Phys. Rev. D **50** (1994) 2199.
- [5] J.F. Gunion, H.E. Haber, and M. Sher, Nucl. Phys. **B306** (1988) 1.
- [6] L. Alvarez-Gaumé and J. Polchinski, Nucl. Phys. **B221** (1983) 495.
- [7] CDF Collaboration, Phys. Rev. Lett. **73** (1994) 225; *ibid.*, “Observation of Top Quark Production in  $\bar{p}p$  Collisions with the CDF Detector at Fermilab”, preprint FERMILAB-PUB-95/022-E, hep-ex/9503002.
- [8] B. Pendleton and G.G. Ross, Phys. Lett. B **98** (1981) 291; C.T. Hill, Phys. Lett. B **98** (1981) 291; V. Barger, M. Berger, P. Ohmann, and R.J.N. Phillips, Phys. Lett. B **314** (1993) 351.
- [9] R. Tarrach, Nucl. Phys. **B183** (1981) 384.
- [10] L.E. Ibáñez and G.G. Ross, Phys. Lett. B **110** (1982) 215; K. Inoue, A. Kakuto, H. Komatsu, and S. Takeshita, Prog. Theor. Phys. **68** (1982) 96; L. Alvarez-Gaumé, M. Claudson, and M.B. Wise, Nucl. Phys. **B207** (1982) 96.
- [11] G. Gamberini, G. Ridolfi, and F. Zwirner, Nucl. Phys. **B331** (1990) 331.
- [12] M. Claudson, J. Hall, and I. Hinchliffe, Nucl. Phys. **B228** (1983) 501.

- [13] Particle Data Group, Phys. Rev. D **50** (1994) 1173.
- [14] W. Siegel, Phys. Lett. B **84** (1979) 193; D.M. Capper, D.R.T. Jones, and P. Nieuwenhuizen, Nucl. Phys. **B167** (1980) 479.
- [15] M.B. Einhorn and D.R.T. Jones, Nucl. Phys. **B230** (1984) 261; H. Nakano and Y. Yoshida, Phys. Rev. D **49** (1994) 5393; C. Ford, *ibid.* 50 (1994) 7531.
- [16] J. Polchinski and M. Wise, Phys. Lett. B **125** (1983) 393.
- [17] E. Weinberg and A. Wu, Phys. Rev. D **36** (1987) 2474.
- [18] W. Press, B. Flannery, S. Teukolsky, and W. Vetterling, *Numerical Recipes - The Art of Scientific Computing*, (Cambridge University Press, Cambridge, 1986).
- [19] J. Ellis, G. Ridolfi, and F. Zwirner, Phys. Lett. B **257** (1991) 83; J. Ellis *et al.*, *ibid.* **262** (1991) 477; A. Brignole, J. Ellis, G. Ridolfi, F. Zwirner, *ibid.* **271** (1991) 123.

TABLES

TABLE I. Grid of parameter values used to calculate the CCB bound for the Lagrangian of Eq. (8).

Parameter	Min. Value	Max. Value	Grid Spacing
$A$	0.0	3.0	0.1
$m_2^2$	-0.250	0.750	0.075
$m_Q^2$	0.0	0.750	0.075
$m_T^2$	0.0	0.750	0.075

TABLE II. CCB bounds for the potential of Eq. (8) with  $h = 0.1$  and  $h = 1.0$ . The coefficients,  $P_i$ , are defined in Eq. (7).

Parameter	$h = 0.1$	$h = 1.0$
$P_1$	0.7246	2.723
$P_2$	0.1608	3.527
$P_3$	-3.808	-8.310
$P_4$	0.1991	3.370
$P_5$	-3.830	-8.228
$P_6$	0.1985	3.452
$P_7$	-3.836	-8.310
$P_8$	0.4911	0.5877
$\langle d^2 \rangle$	$2.8 \times 10^{-4}$	$4.1 \times 10^{-4}$

TABLE III. Grid of parameter values used to calculate the tree-level and one-loop CCB bounds for the MSSM Lagrangian given in the appendix.

Parameter	Min. Value	Max. Value	Tree-level Grid Spacing	One-loop Grid Spacing
$A_t$	0.0	3.0	0.1	0.4
$m_2^2$	$2.5 \times 10^{-3}$	0.7525	0.125	0.25
$m_{\tilde{q}}^2$	$2.5 \times 10^{-3}$	0.7525	0.125	0.25
$m_{\tilde{t}}^2$	$2.5 \times 10^{-3}$	0.7525	0.125	0.25

TABLE IV. Tree-level and one-loop CCB bounds for the MSSM Lagrangian using method S. The coefficients,  $P_i$ , are defined in Eq. (7).

Parameter	tree-level	one-loop
$P_1$	$6.192 \times 10^3$	$5.370 \times 10^1$
$P_2$	$3.078 \times 10^3$	$1.203 \times 10^1$
$P_3$	$-3.107 \times 10^3$	$-4.913 \times 10^0$
$P_4$	$6.721 \times 10^3$	$6.872 \times 10^1$
$P_5$	$-1.162 \times 10^4$	$-1.120 \times 10^2$
$P_6$	$6.857 \times 10^3$	$7.268 \times 10^1$
$P_7$	$-1.175 \times 10^4$	$-1.068 \times 10^2$
$P_8$	$-1.305 \times 10^3$	$-1.233 \times 10^1$
$\langle d^2 \rangle$	$1.2 \times 10^{-3}$	$4.8 \times 10^{-3}$

TABLE V. Tree-level and one-loop CCB bounds for the MSSM Lagrangian using method F.

The coefficients,  $P_i$ , are defined in Eq. (7).

Parameter	tree-level	one-loop
$P_1$	$4.431 \times 10^2$	$3.000 \times 10^0$
$P_2$	$9.397 \times 10^2$	$-1.307 \times 10^1$
$P_3$	$-1.452 \times 10^3$	$5.948 \times 10^0$
$P_4$	$3.478 \times 10^2$	$7.767 \times 10^0$
$P_5$	$-6.650 \times 10^2$	$-9.086 \times 10^0$
$P_6$	$3.553 \times 10^2$	$-7.102 \times 10^0$
$P_7$	$-6.700 \times 10^2$	$3.374 \times 10^0$
$P_8$	$-2.346 \times 10^2$	$-2.833 \times 10^{-1}$
$\langle d^2 \rangle$	$1.6 \times 10^{-3}$	$9.4 \times 10^{-3}$

## FIGURES

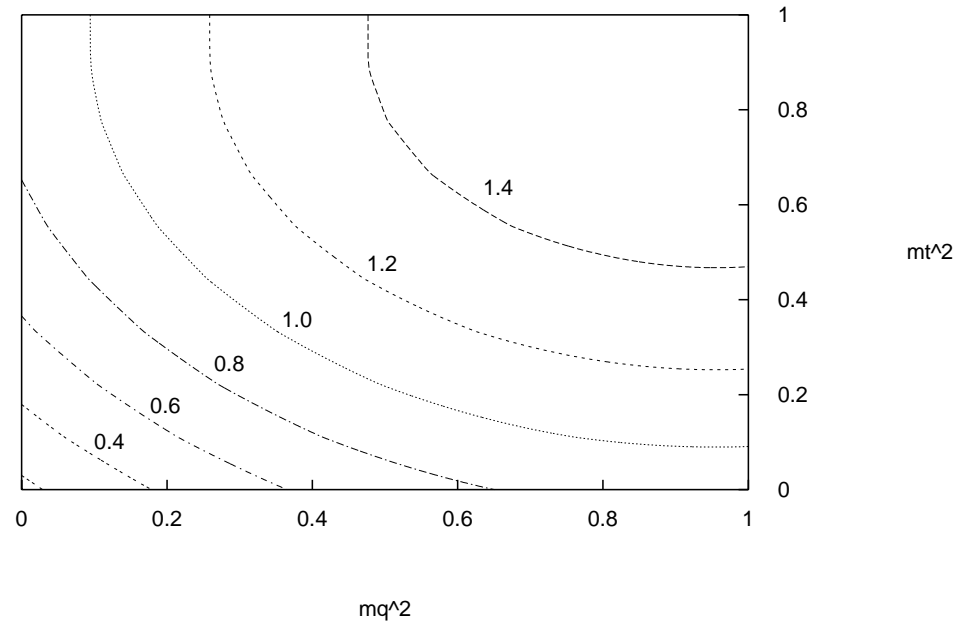


FIG. 1. Tree-level CCB bound for method F given in Table V.  $m_2^2 = 0.25$  and each contour is labeled with the corresponding maximum  $A$  value.

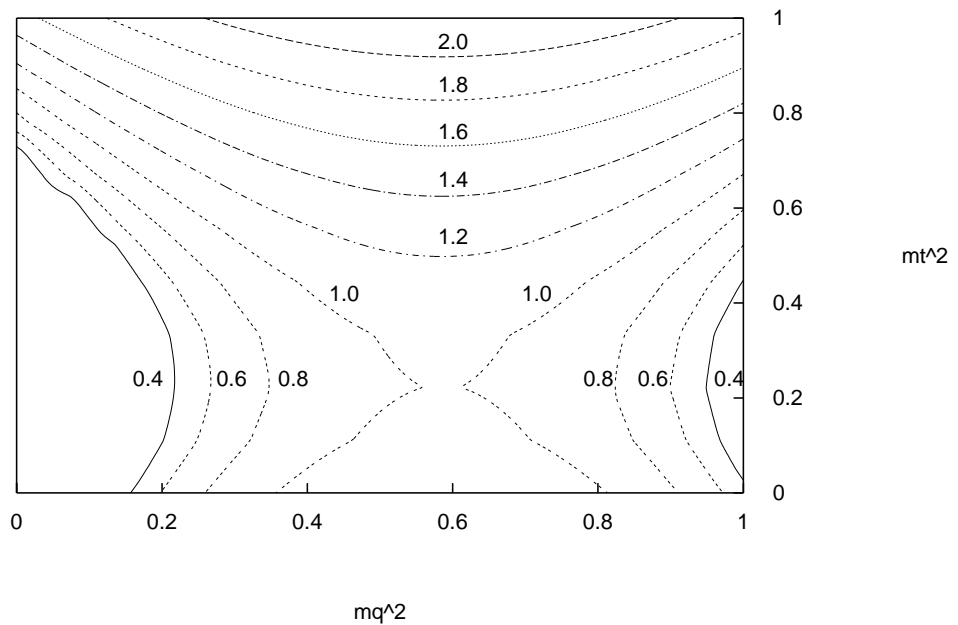


FIG. 2. One-loop CCB bound for method F given in Table V.  $m_2^2 = 0.25$  and each contour is labeled with the corresponding maximum  $A$  value.

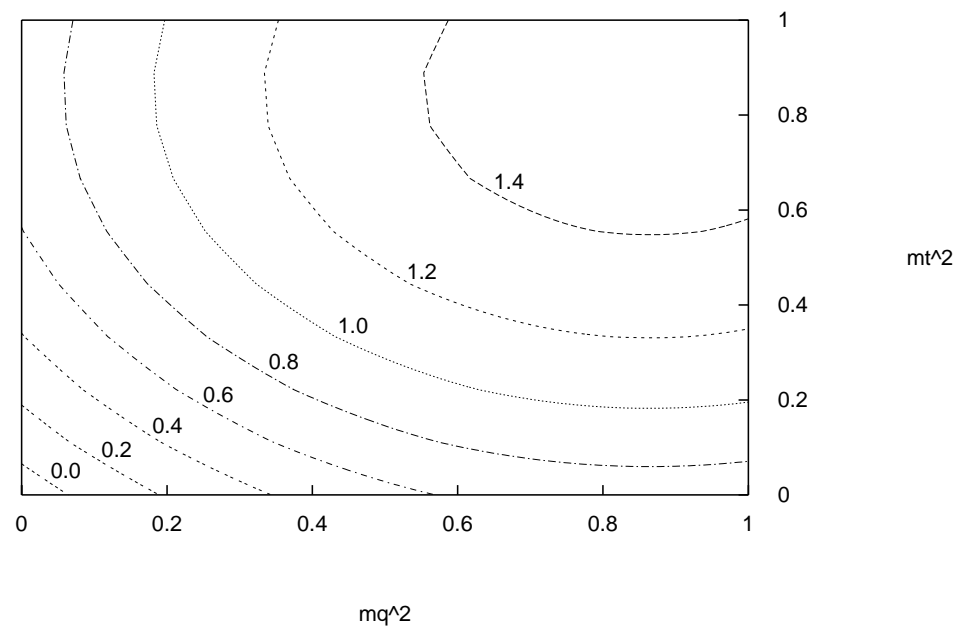


FIG. 3. Tree-level CCB bound for method S given in Table IV.  $m_2^2 = 0.25$  and each contour is labeled with the corresponding maximum  $A$  value.

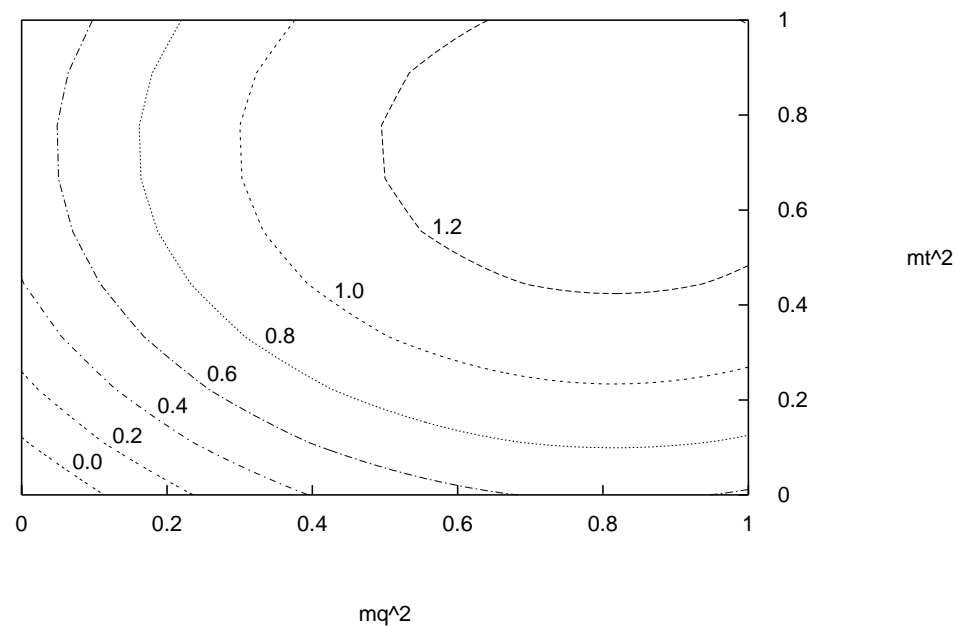


FIG. 4. One-loop CCB bound for method S given in Table IV.  $m_2^2 = 0.25$  and each contour is labeled with the corresponding maximum  $A$  value.

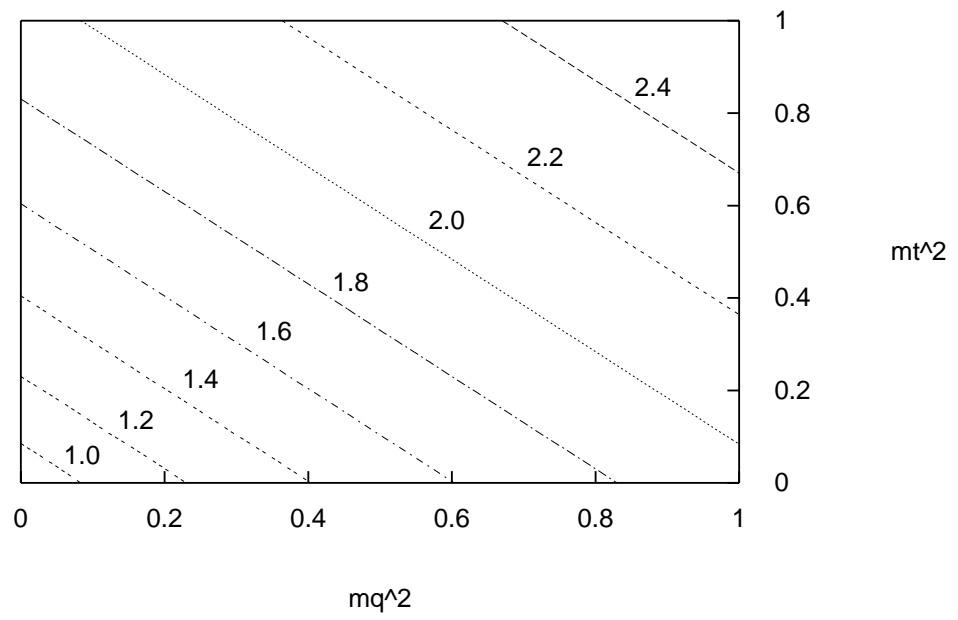


FIG. 5. Analytical CCB bound for the potential of Eq. (8) given in Eq. (9).  $m_2^2 = 0.25$  and each contour is labeled with the corresponding  $A$  value.